

# Image Dehazing with Dark Channel Prior and Novel Estimation Model

Bingquan Huo and Fengling Yin

*Binzhou Polytechnic, Shandong, China*  
*bingquanhuo666@126.com*

## **Abstract**

*Single Image Dehazing technology is widely needed in many fields. In order to solve the problem, we propose an improved and modified framework for estimating the optical transmission  $t$  in hazy scenes in a given single input image. At first, a novel formulation to the  $t$  estimation is presented with the combination of constant albedo and dark channel prior knowledge. Later, we introduce the watershed segmentation methodology into the algorithm to separate the image into some gray level consistent parts based on the original image's color distribution and feature difference. As a result, we could estimate the atmospheric light  $A$  better and avoid the important drawback of artifacts phenomenon. At last, through this effective estimation to  $t$  and  $A$ , the scene visibility is largely increased and the haze-free scene contrasts can be better recovered. The experimental analysis shows that compared with other state-of-the-art algorithms, our proposed algorithm can provide promising results to dark channel prior and get corresponding reliable estimation value  $t$  with the advantage of minimal halo artifacts and fewer unreal details. Our method is more effective and robust.*

**Keywords:** *Image Segmentation, Dark Channel Prior, Image Dehaze, Estimation Model*

## **1. Introduction**

Image dehazing as one of the most important research areas and basic issues in the community of image processing and pattern analysis, the ultimate image dehazing goal can be summarized as two aspects. One is creating visually pleasing images suitable for human visual perception whereas the other is to improve the interpretability of images for computer vision and preprocessing tasks. Therefore, effective and robust algorithms and techniques for image dehazing are urgently needed. Due to the presence of aerosols such as dust, mist, and fumes which deflect light from its original course of propagation, the light reflected from a surface is scattered in the atmosphere before it reaches the camera in almost every practical scenario. Furthermore, the degradation would be more serious with increasing of the distance between camera and object. Removing haze can not only significantly increase the visibility of the scene and correct the color shift caused by the atmospheric light, which makes the image much more visually pleasing, it can also be used for computer vision algorithms to analyze low-level image and high-level object recognition. Besides, in many computer vision algorithms and advanced image editing, haze removal can play an important role in producing depth information. Thus, haze removal has been more and more highly valued recently. However, single image haze removal is a challenging problem because it is very difficult to get depth from a single image.

However, single image haze removal is a challenging problem because it is very difficult to get depth from a single image. Some methods are proposed using multiple images [1,2,3,4,5]. The basic idea is to exploit the differences between multiple images

captured for the same scene under different atmosphere. A single image dehazing research has made significant progress in recent years. Dong Nan [10] proposed a novel Bayesian framework for single image dehazing considering noise, at first the Bayesian framework is transformed to meet the dehazing algorithm. Then, the probability density function of the improved atmospheric scattering model is estimated by using the statistical prior and objective assumption of degraded image. Finally, the reflectance image is achieved by an iterative approach with feedback to reach the balance between dehazing and denoising. R. Tan [6] pointed out that the haze-free image must have a higher contrast ratio and input image of haze. He removes the haze, maximize the local contrast of image. In addition, he also puts forward the assumption adjacent pixels suffer the same degradation, and the optimal method based on markov random field is used to eliminate the haze. The method in practice, however, may lead to the over - enhanced image. Under the assumption that the transmission and surface shading are locally uncorrelated, Fattal [7] uses Independent Component Analysis to estimate the transmission, and then infers the medium transmission and the color of the whole image by MRF. Fattal's approach is physically sound and can produce impressive results, but has difficulty with scenes involving fog, as the magnitude of the surface reflectance is much smaller than that of the atmospheric light when the fog is suitably thick. In fact, when the assumption is broken, this method may be failed. Schechner's approach [8] focuses on the analysis of images taken through a polarizer. Polarization filtering has long been used in photography through haze [5]. However, it is restrictive to rely only on optical filtering because it can work well on clear days. In the situations with weak light scattering (mainly due to air molecules), photographers set the polarization filter at an orientation that best improves image contrast. In general, however, polarization filtering alone cannot remove the haze from images well. According to dark channel prior and a common haze imaging model, Long [11] use a low-pass Gaussian filter to refine the coarse estimated atmospheric veil. Later, redefine the transmission, with the aim of preventing the color distortion of the recovered images. The main advantage of the proposed algorithm is its fast speed, while it can also achieve good results. Based on the statistics of haze-free outdoor images, He *et al.* [9] employs a dark channel prior which assumes some pixels (called "dark pixels") have very low intensity in at least one color (RGB) channel in most of the local regions which do not cover the sky. A soft matting algorithm is used to refine the transmission. Although it is computational expensive, it work well in the final result. This approach is physically valid and is able to handle distant objects even in the heavy haze image. It does not rely on significant variance on transmission or surface shading in the input image. However, the result contains few halo artifacts. Furthermore, in the situation that the scene object is inherently similar to the atmospheric light over a large local region, especially when no shadow is cast on the object, the color of the output images is likely to be changed, which is a weakness of this approach.

## 2. The Current Models

### 2.1. The Optical Model

In surveillance, intelligent vehicles and remote sensing systems, the image appearance is subject to weather conditions such as the influences of haze, fog and smoke. On a gray level image, the optical model is established by Koschmieder as the following relationship [12] based on physical properties of light transmission in atmosphere.

$$I(x) = J(x)t(x) + A(1-t(x))$$

(1)

Where  $I(x)$  represents the apparent luminance at the pixel  $x$  and  $t(x) = e^{-\beta d(\lambda)}$  is the transmission process of the map.  $d(\lambda)$  is the distance of the corresponding object with intrinsic luminance  $J(x)$ .  $A$  is the luminance of the sky and  $\beta$  denotes the extinction coefficient of the atmosphere. In Equation (1), the first term  $J(x)t(x)$  is called direct attenuation, and the second term  $A(1-t(x))$  is called atmospheric light. This Optical model is directly extended to each RGB component of a color image by assuming a camera with a linear response.

## 2.2. The Dark Channel Prior Model

According to the literature report [9], based on the observation on haze-free outdoor images, in most of the non-sky patches, at least one color channel has very low intensity at some pixels, which is called the dark channel prior (DCP). In another word, the minimum intensity in such a patch should have a very low value. The general definition and principle of the dark channel prior used for image dehazing is formulated as the following:

$$\theta_D(m, n) = \min_{k, l \in \Omega_x(m, n)} \left( \min_{c \in \{r, g, b\}} \frac{x(k, j, c)}{a(c)} \right) \quad (2)$$

Therefore, the dark channel prior gets the least distance to the Lowner-John ellipsoid which could be defined as the following formula 3.

$$\theta_D(m, n) \square \begin{cases} \arg \min_{c, z} & \|z_c - y\|_2 \\ \text{subject to} & z_c^T e_c = 0 \\ \text{and} & y^T A^{-1} y = 1 \end{cases} \quad (3)$$

The  $e_c$  denoted as the unit vector is the representative of the normal to one of the 3-dimensional color regulation within the color cube of RGB,  $A$  as the parameter of specific matrix comes from the Lowner- John ellipsoid. On the condition that the light is colorless,  $a = \alpha 1_p$ , for  $0 < \alpha \leq 1$ , we could therefore get the revised version of formula 2 as the following:

$$\theta_D(m, n) = \frac{1}{\alpha} \min_{k, l \in \Omega_x(m, n)} \left( \min_{c \in \{r, g, b\}} x(k, j, c) \right) \quad (4)$$

As far as the transmission is concerned, the following formulas express the detailed procedure:

$$t_D(m, n) = 1 - w\theta_D(m, n) \geq 1 - w\theta_E(m, n) = t_E(m, n) \quad (5)$$

$t_D$  and  $t_E$  denoted as the function of transmission are the EP and dark channel prior estimation of transmission constructed in the same fashion with the weighting value parameter set to  $w = 0.95$ , respectively.

### 2.3. The Constant Albedo Model

According to [7], Fattal assumes the unknown image  $J$  as a pixel wise product of surface albedo coefficients and a shading factor, where is a three-channel RGB vector of surface reflectance coefficients and is a scalar describing the light reflected from the surface. The model is refined by assuming that is piecewise constant. At these pixels, the optical model becomes:

$$I(x) = t(x)l(x)R + A(1-t(x)) \quad (6)$$

Then he proceeds by breaking  $R$  into a sum of two components, one parallel to the atmospheric light  $A$  and a residual vector  $A^\perp$ . In terms of these normalized components, he projects the input image along and perpendicular to the atmospheric light vector, which results in a scalar given by

$$I_A(x) = t(x)l'(x)\eta + (1-t(x))\|A\| \quad (7)$$

$$I_R(x) = t(x)l'(x) \quad (8)$$

$I_A(x)$  and  $I_R(x)$  are the representation of components parallel and vertical to atmospheric light and generally  $\eta = C_\Omega(I_A, h)/C_\Omega(I_R, h)$ . With the above discussion and analysis, we can define the transmission function as:

$$t(x) = 1 - \frac{1}{\|A\|} (I_A(x) - \eta I_R(x)) \quad (9)$$

## 3. The Proposed Model

### 3.1. The Estimation of Transmission

According to He and Fattal's assumptions:

$$J^{dark}(x) = \text{Min}_{c \in \{r, g, b\}} \left[ \text{Min}_{y \in \Omega(x)} (J^c(y)) \right] = \text{Min}_{c \in \{r, g, b\}} \left[ \text{Min}_{y \in \Omega(x)} (l(y)R) \right] \quad (10)$$

And combine with formula 6, the following equation could be derived:

$$\text{Min}_{c \in \{r, g, b\}} \left[ \text{Min}_{y \in \Omega(x)} (J^c(y)) \right] = \text{Min}_{c \in \{r, g, b\}} \left[ \text{Min}_{y \in \Omega(x)} (l(y)R) \right] = \text{Min}_{c \in \{r, g, b\}} (R) \text{Min}_{y \in \Omega(x)} (l(y)) = 0 \quad (11)$$

Then the equation 11 can be classified into the following two different conditions.

#### 3.1.1. The Condition One

Generally,  $l' = \|R\|l$ . and, As we have known that  $I_A(x)$  and  $I_R(x)$  are scalars. Therefore it can be inferred that:

$$\min_{y \in \Omega(x)} I_A(y) = \min_{y \in \Omega(x)} \left[ (1-t(y))\|A\| \right] \quad (12)$$

$$\min_{y \in \Omega(x)} I_R(x) = \min_{y \in \Omega(x)} (t(x)l'(x)) = 0 \quad (13)$$

$$\frac{\langle I, A \rangle}{\|A\|} = \frac{\langle A, J \rangle t(x)}{\|A\|} + (1-t(x))\|A\| \quad (14)$$

And then we can further assume that the *transmission* in a local patch  $\Omega(x)$  is constant. Then we get an estimation of *transmission*:

$$t(x) = 1 - \frac{\langle I(x), A \rangle}{\|A\|^2} \quad (15)$$

Since the haze exists in practice, especially when we look at distant objects. It is reasonable to add some haze in the final result to make the image more natural. Thus the *transmission* can be refined as:

$$t(x) = 1 - w \frac{\langle I(x), A \rangle}{\|A\|^2} \quad (16)$$

Where  $w(0 < w < 1)$  is a constant. The value of  $w$  is based on application. In this paper, we fix it to 0.95 in most of the results.

### 3.1.2. The Condition Two

In the condition, the prior requirement is that:

$$\min\{R^c \mid c \in \{r, g, b\}\} = 0. \quad (17)$$

Since is constant in local patches, this condition can only be discussed in some special situations such as the reflection of grass.

### 3.2. The Halo Artifacts Removal with Image Segmentation

As described previously, the *transmission* map can be obtained by specifying the global atmospheric light. In this paper, we adopt the approach in the previous discussion to estimate  $A$ . With the *transmission* map, the haze-free image can be recovered according to equation (1). However, a problem is found that there are halo artifacts at the depth-discontinuous edges as shown in Figure 1(b). Since the depth is usually assumed to be the same in every given  $15 \times 15$  patch, halo artifacts is unavoidable because in the patch there are always erupt changes of color in the same patch. Thus the selection of patch region is unreasonable.

In this paper, we introduce the watershed segmentation to solve the problem instead of dealing with it by dividing the whole image into some  $15 \times 15$  patches as shown in Figure 1(d). By using the watershed segmentation algorithm, we can calculate the atmospheric light and dark-channel of input image and the *transmission* (Figure 1(c)) is assumed to be a constant in regions of segmentation. This method can reduce the erupt changes in depth-discontinuous edges which result in halo artifacts. In many cases, the region, may produce too much calculation produces a great burden. Control the amount of calculation, we introduce several parameters:  $\sigma$  and  $\min$ , where  $\sigma$  is the Watershed ridge pixels that control segmentation and  $\min$  is the minimum size of each patch.

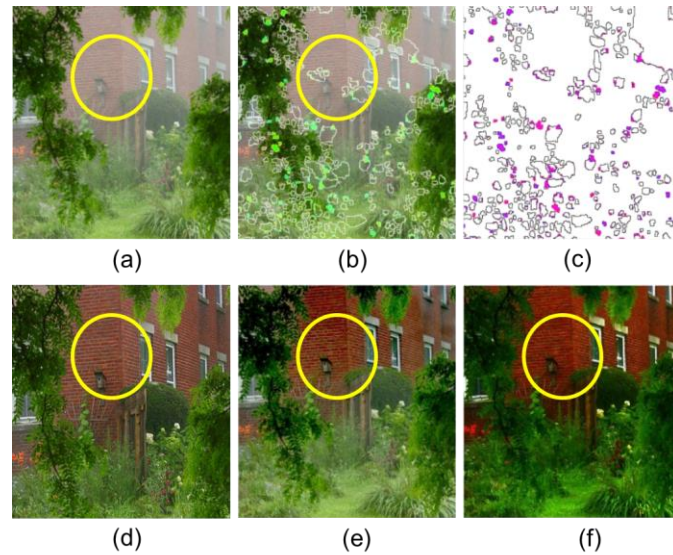


**Figure 1. (a) The Input Image (b) Segmentation Result with the Scene (c) Segmentation Result without the Scene (d) He's Result (e) Fattal's Result (f) Our result**

### 3.3. Estimating the Atmospheric Light

In this paper, we improve He's approach to estimate atmospheric light  $A$ . According to He's algorithm, his approach works well when/based on the assumption that there is some sky region which is used to estimate the  $A$  and the magnitude of area of sky cannot be very large in the given image. Follow the above assumptions, the top part of the picture, we think that can better estimate the atmospheric light, because if there is the sky area image, it is always in the part of the image, and if not, we can estimate the atmospheric light the sky area does not exist. So if we estimate the atmospheric light and the whole image, it may affect the outcome. In addition, it also can reduce the amount of calculation. However, the atmospheric light color can also be changed in the image if the range of vision is too large. In such situations, the segmentation in the previous section can be adopted to solve the problem. We divide the whole image into several parts and estimate the atmospheric light in the top area (as shown in Figure 1 (c)). By this approach, the dehazing result can be improved.

To control the result of division, there are several parameters:  $\max$  and  $k$ , where  $\max$  is the maximum number of all parts and  $k$  is a constant to constrain the area of top part. From each area of the segmentation, we pick the top 0.1% brightest pixels in the dark channel. Then we compute their average as the value of the atmospheric light  $A$  in the whole image.

## 4. The Experimental Analysis

In our proposed method, we introduce the Watershed algorithm [9] to conduct region division to single hazy image. And use the transmission map to calculate the transmission values of different regions. Our method mainly includes the following four steps: region division, computing transmission map, atmospheric light estimation and image dehazing. Parameters in the algorithm are initialized as follows: The algorithm is implemented on a P4-4GHz PC with 2 GB RAM. It takes about 10-20seconds to process a 600\*400 pixels image. Fig. 2 (e) and (f) show our haze removal results with different. The atmospheric lights in the input image are estimated by using our proposed method described in Section

3.3. From fig. 2(f), it can be seen that our method significantly overcomes the dense fog and recovers most detail. Besides, the estimated depth maps are sharp and consistent with the input images. Compared with *He's* results in Figure 1, our approach performs better in halo artifacts. It is shown that the light is clearer when  $\omega = 0.9$  or  $0.95$ .

In Figure 3, we compare our approach with *Tan's* work. The colors of his result are often over saturated, since his algorithm is not based on physical and may underestimate the *transmission*. Our method recovers the structures without sacrificing the fidelity of the colors (e.g., the swans in the image). Although in some part of the image, the details ((e.g., the trees in the right of image)) cannot be recovered totally, the color of the whole image is more real in our result. Fig. 4 (b-e) stands for haze removal results by *Fattal*, *Tan*, *Koph* and our method, respectively. Fig. 4 (f) is the revised *transmission* map of the input image. From Fig.4 (b), Due to *Fattal's* method is based on statistics results and requires sufficient color information especially variance of color, *Fattal's* approach has some difficulties in recovering the hazy image under the dense haze. With the dense haze, the color of the hazy image is basically uniform and its variance is not high enough, which make it difficult to reliably estimate the *transmission*. Besides, in Fig.4 (c), *Tan's* result shows the problem of over saturating. In comparison, our approach can recover more details of scenarios as shown in Fig. 4(e).

The comparison result with *Koph's* is shown in Fig.4(d). *Koph's* method, which incorporates the 3D geography information, can perform well in the recovery of the hazy image, but it cannot be applied widely Because of its requirement of a huge amount of information. On the contrary, our result can recover sufficient details and use less information.

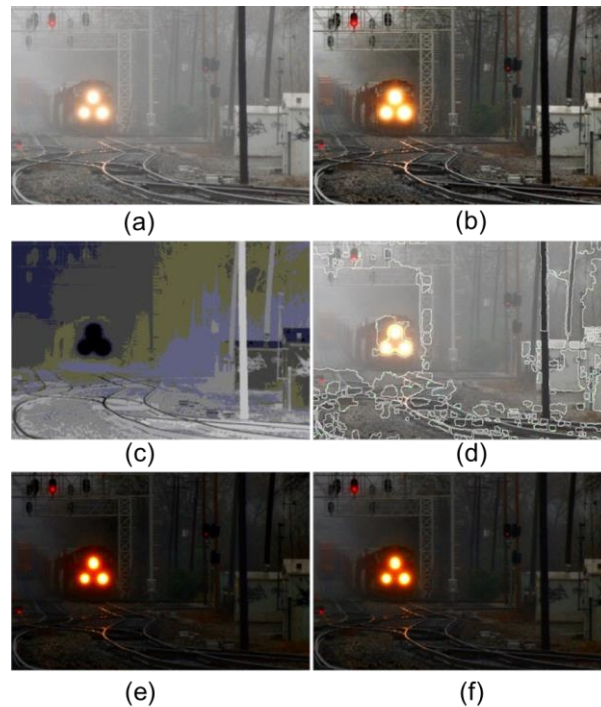


**Figure 2. (a) The Input Image (b) Fattal's Result (c) The Revised Transmission Map (d) Segmentation with the Scene (e,f) Our Results**



**Figure 3. Comparison with Tan's Work**

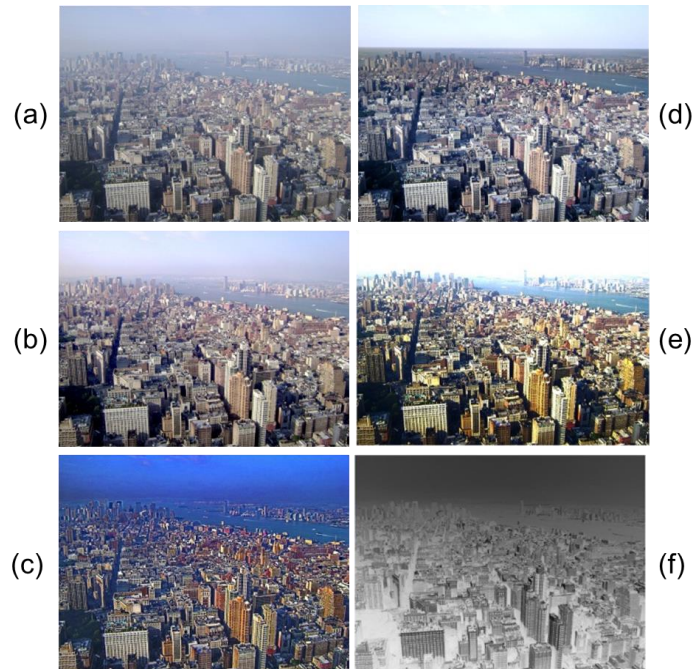


**Figure 4. (a) The Input Image (b) Fattal's Result (c) Tan's Result (d) Koph et al.'s Result (e) Our Result with (f) The Revised Transmission Map**

## 5. Conclusion and Summary

This paper presents a new approach to estimate transmission by combining statistical results and dark-channel. This approach enables dehazing when the problem cannot be solved by optics alone. In addition to statistical results and optics, segmentation is proved a better way to divide the whole image than a  $15 \times 15$  patch region. Our method is based on the partial estimation of atmospheric light. Therefore, its stability will decrease as the accuracy of segmentation decreases. For instance, the method may fail in situations of fog or very dense haze since in such situation it may be difficult to divide the image accurately. Besides, since the errors in the dark channel prior still remains, our method can only solve the problem to some extent when color of the scene object is similar to the atmospheric light. Future work will try to figure out a better way to estimate atmospheric light to solve the problem that the color of the image is changed to some extent (e.g., Figure 4 (e)). In addition, some reverse problem based mathematical tools are still needed such as the literatures of [13-20]. Image dehazing issue in urgently needed to be dealt with and find out for a more robust and effective solution.



## References

- [1] K. He, J. Sun, and X. Tang, "Single image haze removal using dark channel prior", *Pattern Analysis and Machine Intelligence*, IEEE Transactions, (2011), pp. 2341-2353.
- [2] C. O. Ancuti and C. Ancuti, "Single image dehazing by multi-scale fusion", *Image Processing*, IEEE Transactions, (2013), pp. 3271-3282.
- [3] Y. Yang, *et al.*, "A novel single image dehazing method", *Computational Problem-solving (ICCP)*, 2013 International Conference, (2013).
- [4] X. Lu, G. Lv, and T. Lei, "Single image dehazing based on multiple scattering model", *Signal Processing, Communications and Computing (ICSPCC)*, 2014 IEEE International Conference on. IEEE, (2014).
- [5] S. Tao, *et al.*, "Single image dehazing based on dark channel prior", *Seventh International Symposium on Multispectral Image Processing and Pattern Recognition (MIPPR2011)*, International Society for Optics and Photonics, (2011).
- [6] R.T. Tan, "Visibility in bad weather from a single image," *IEEE Conference on Computer Vision and Pattern Recognition*, pp. 1–8, (2008).
- [7] R. Fattal, "Single image dehazing", *International Conference on Computer Graphics and Interactive Techniques*, (2008), pp. 1–9.
- [8] Y.Y. Schechner, S.G. Narasimhan, and S.K. Nayar, "Instant dehazing of images using polarization", *IEEE Conference on Computer Vision and Pattern Recognition*, (2001), pp. 325-332.
- [9] J. A. Valderrama, V. H. Diaz-Ramirez and V. Kober, "Single image dehazing using local adaptive signal processing", *SPIE Optical Engineering+ Applications*, International Society for Optics and Photonics, (2014).
- [10] D. Nan, *et al.* "A Bayesian Framework for Single Image Dehazing considering Noise", *The Scientific World Journal* 2014, (2014).
- [11] J. Long, *et al.* "Single Remote Sensing Image Dehazing", *Geoscience and Remote Sensing Letters*, IEEE 11.1, (2014), pp. 59-63.
- [12] N. Hautiere, J.-P. Tarel, J. Lavenant, and D. Aubert, "Automatic fog detection and estimation of visibility distance through use of an onboard camera", *Machine Vision and Applications*, vol. 17, no. 1, (2006), pp. 8–20.
- [13] A. J. Davies, *et al.* "Reverse differentiation and the inverse diffusion problem", *Advances in Engineering Software*, vol. 28, no. 4, (1997), pp. 217-221.
- [14] M. R. Eden, *et al.*, "Reverse problem formulation based techniques for process and product synthesis and design", *Computer Aided Chemical Engineering*, vol. 15, (2003), pp. 451-456.
- [15] E. M. Lovelady, *et al.* "Reverse problem formulation for integrating process discharges with watersheds and drainage systems", *Journal of Industrial Ecology*, vol. 13, no. 6, (2009), pp. 914-927.
- [16] N. G. Chemmangattuvalappil, *et al.* "Reverse problem formulation approach to molecular design using property operators based on signature descriptors", *Computers & Chemical Engineering*, vol. 34, no. 12, (2010), pp. 2062-2071.
- [17] M. Dao, *et al.*, "Computational modeling of the forward and reverse problems in instrumented sharp indentation", *Acta materialia*, vo. 49, no. 19, (2001), pp. 3899-3918.
- [18] Y. Zhang and J. Sun, "Practical issues of reverse time migration-true-amplitude gathers, noise removal and harmonic-source encoding", *70th EAGE Conference & Exhibition*, (2008).
- [19] D. A. Qing-li, Z.-Q. Huang, and Q. Zhang, "Current and Future Studies on Structure of the Reverse Logistics System: A Review", *Chinese Journal of Management Science*, vol. 1, (2004), p. 024.
- [20] R. Sikora and R. Palka, "Reverse problems for diffusion equation", *Electrical Engineering (Archiv fur Elektrotechnik)*, vol. 62, no. 3, (1980), pp. 177-180.

